Microcavity enhanced optical absorption in subwavelength slits

Changjun Min,[1] Liu Yang,[2] and Georgios Veronis[1,2,*]

[1]*Center for Computation and Technology, Louisiana State University, Baton Rouge, Louisiana 70803, USA*
[2]*Department of Electrical and Computer Engineering, Louisiana State University, Baton Rouge, Louisiana 70803, USA*
[*]*gveronis@lsu.edu*

Abstract: We introduce a compact submicron structure consisting of multiple optical microcavities at both the entrance and exit sides of a subwavelength plasmonic slit filled with an absorbing material. We show that such microcavity structures at the entrance side of the slit can greatly enhance the coupling of the incident light into the slit, by improving the impedance matching between the incident plane wave and the slit mode. In addition, the microcavity structures can also increase the reflectivities at both sides of the slit, and therefore the resonant field enhancement. Thus, such structures can greatly enhance the absorption cross section of the slit. An optimized submicron structure consisting of two microcavities at each of the entrance and exit sides of the slit leads to ~9.3 times absorption enhancement at the optical communication wavelength compared to an optimized slit without microcavities.

OCIS codes: (240.6680) Surface plasmons; (260.3910) Metal optics; (260.5740) Resonance.

References and links

1. T. W. Ebbesen, H. J. Lezec, H. F. Ghaemi, T. Thio, and P. A. Wolff, "Extraordinary optical transmission through sub-wavelength hole arrays," Nature **391**(6668), 667–669 (1998).
2. T. Thio, K. M. Pellerin, R. A. Linke, H. J. Lezec, and T. W. Ebbesen, "Enhanced light transmission through a single subwavelength aperture," Opt. Lett. **26**(24), 1972–1974 (2001).
3. H. J. Lezec, A. Degiron, E. Devaux, R. A. Linke, L. Martin-Moreno, F. J. Garcia-Vidal, and T. W. Ebbesen, "Beaming light from a subwavelength aperture," Science **297**(5582), 820–822 (2002).
4. F. J. García-Vidal, H. J. Lezec, T. W. Ebbesen, and L. Martín-Moreno, "Multiple paths to enhance optical transmission through a single subwavelength slit," Phys. Rev. Lett. **90**(21), 213901 (2003).
5. W. L. Barnes, A. Dereux, and T. W. Ebbesen, "Surface plasmon subwavelength optics," Nature **424**(6950), 824–830 (2003).
6. D. C. Skigin and R. A. Depine, "Transmission resonances of metallic compound gratings with subwavelength slits," Phys. Rev. Lett. **95**(21), 217402 (2005).
7. C. Genet and T. W. Ebbesen, "Light in tiny holes," Nature **445**(7123), 39–46 (2007).
8. F. J. García-Vidal, L. Martín-Moreno, T. W. Ebbesen, and L. Kuipers, "Light passing through subwavelength apertures," Rev. Mod. Phys. **82**(1), 729–787 (2010).
9. Z. Yu, G. Veronis, S. Fan, and, M. L. Brongersma "Design of mid-infrared photodetectors enhanced by surface plasmons on grating structures," Appl. Phys. Lett. **89**(15), 151116 (2006).
10. J. S. White, G. Veronis, Z. Yu, E. S. Barnard, A. Chandran, S. Fan, and M. L. Brongersma, "Extraordinary optical absorption through subwavelength slits," Opt. Lett. **34**(5), 686–688 (2009).
11. L. Martín-Moreno, F. J. García-Vidal, H. J. Lezec, A. Degiron, and T. W. Ebbesen, "Theory of highly directional emission from a single subwavelength aperture surrounded by surface corrugations," Phys. Rev. Lett. **90**(16), 167401 (2003).
12. F. López-Tejeira, S. G. Rodrigo, L. Martin-Moreno, F. J. García-Vidal, E. Devaux, T. W. Ebbesen, J. R. Krenn, I. P. Radko, S. I. Bozhevolnyi, M. U. Gonzalez, J.-C. Weeber, and A. Dereux, "Efficient unidirectional nanoslit couplers for surface plasmons," Nat. Phys. **3**(5), 324–328 (2007).
13. T. Ishi, J. Fujikata, K. Makita, T. Baba, and K. Ohashi, "Si nano-photodiode with a surface plasmon antenna," Jpn. J. Appl. Phys. **44**(12), L364–L366 (2005).
14. W. Cai, J. S. White, and M. L. Brongersma, "Compact, high-speed and power-efficient electrooptic plasmonic modulators," Nano Lett. **9**(12), 4403–4411 (2009).
15. G. Gbur, H. F. Schouten, and T. D. Visser, "Achieving superresolution in near-field optical data readout systems using surface plasmons," Appl. Phys. Lett. **87**(19), 191109 (2005).
16. J. Fujikata, T. Ishi, H. Yokota, K. Kato, M. Yanagisawa, M. Nakada, K. Ishihara, K. Ohashi, T. Thio, and R. A. Linke, "Surface plasmon enhancement effect and its application to near-field optical recording," Trans. Magn.

#156509 - $15.00 USD Received 13 Oct 2011; revised 8 Dec 2011; accepted 8 Dec 2011; published 15 Dec 2011

Soc. Jpn **4**, 255–259 (2004).
17. S. Shinada, J. Hashizume, and F. Koyama, "Surface plasmon resonance on microaperture vertical-cavity surface-emitting laser with metal grating," Appl. Phys. Lett. **83**(5), 836–838 (2003).
18. B. Guo, G. Song, and L. Chen, "Plasmonic very-small-aperture lasers," Appl. Phys. Lett. **91**(2), 021103 (2007).
19. L. Verslegers, Z. Yu, P. B. Catrysse, and S. Fan, "Temporal coupled-mode theory for resonant apertures," J. Opt. Soc. Am. B **27**(10), 1947–1956 (2010).
20. Q. Min and R. Gordon, "Surface plasmon microcavity for resonant transmission through a slit in a gold film," Opt. Express **16**(13), 9708–9713 (2008).
21. L. Cao, J. S. Park, P. Fan, B. Clemens, and M. L. Brongersma, "Resonant germanium nanoantenna photodetectors," Nano Lett. **10**(4), 1229–1233 (2010).
22. G. Veronis and S. Fan, "Overview of simulation techniques for plasmonic devices," in *Surface Plasmon Nanophotonics*, Mark L. Brongersma and Pieter G. Kik, eds. (Springer, 2007).
23. E. D. Palik, *Handbook of Optical Constants of Solids* (Academic, New York, 1985).
24. J. Jin, *The Finite Element Method in Electromagnetics* (Wiley, New York, 2002).
25. A. Taflove and S. C. Hagness, *Computational Electrodynamics: The Finite-Difference Time-Domain Method*, 3rd ed., (Artech House, Norwood, 2005).
26. S. E. Kocabas, G. Veronis, D. A. B. Miller, and S. Fan, "Transmission line and equivalent circuit models for plasmonic waveguide components," IEEE J. Sel. Top. Quantum Electron. **14**(6), 1462–1472 (2008).
27. K. Krishnakumar, "Micro-genetic algorithms for stationary and non-stationary function optimization," Proc. SPIE **1196**, 289–296 (1989).
28. G. Veronis and S. Fan, "Theoretical investigation of compact couplers between dielectric slab waveguides and two-dimensional metal-dielectric-metal plasmonic waveguides," Opt. Express **15**(3), 1211–1221 (2007).

1. Introduction

Following the observation of extraordinary optical transmission through arrays of subwavelength apertures in metallic films [1], there has been enormous interest in the properties of plasmonic structures consisting of subwavelength apertures [2–8]. Resonant subwavelength plasmonic apertures can efficiently concentrate light into deep subwavelength regions, and therefore significantly enhance the optical transmission through the apertures [3–8], or the absorption in the apertures [9,10]. In addition, grating structures, consisting of periodic arrays of grooves patterned on the metal film surrounding the aperture, are commonly used to enhance the coupling of incident light into the aperture through the excitation of surface plasmons [3,7,9,11–18]. For efficient surface plasmon excitation, however, the period of the grating has to be equal to the surface plasmon wavelength, and several grating periods are required. Thus, such structures need to be several microns long to operate at optical frequencies.

In this paper, we show that a compact submicron structure consisting of multiple optical microcavities at both the entrance and exit sides of a subwavelength plasmonic slit filled with an absorbing material can greatly enhance the absorption cross section of the slit. Our reference structure is a single optimized subwavelength slit in a metal film deposited on a substrate. We show that such microcavity structures at the entrance side of the slit can greatly enhance the coupling of the incident light into the slit, by improving the impedance matching between the incident plane wave and the slit mode. In addition, the microcavity structures can increase the reflectivities at both sides of the slit, and therefore the resonant field enhancement in the slit. An optimized submicron structure consisting of two microcavities at each of the entrance and exit sides of the slit leads to ~9.3 times absorption enhancement at the optical communication wavelength compared to the optimized reference slit without microcavities. We also show that, while the microcavity enhanced structures are optimized at a single wavelength, the operation wavelength range for high absorption is broad.

In previous studies, it was demonstrated that the use of a single microcavity at the entrance and exit sides of a subwavelength slit, can enhance the transmission cross section of the slit [19,20].

The remainder of the paper is organized as follows. In Section 2, we define the absorption cross section and absorption enhancement factor of the slit, and employ single-mode scattering matrix theory to account for their behavior. The results obtained for the reference structure of a slit without microcavities, as well as for the microcavity enhanced structures are presented in Section 3. Finally, our conclusions are summarized in Section 4.

#156509 - $15.00 USD Received 13 Oct 2011; revised 8 Dec 2011; accepted 8 Dec 2011; published 15 Dec 2011

2. Absorption cross section and absorption enhancement factor

We consider a structure consisting of a single slit in a silver film with N microcavities at the entrance side, and M microcavities at the exit side of the slit deposited on a silica substrate (Fig. 1(a)). The slit is filled with germanium, which is one of the most promising materials for near-infrared photodetectors in integrated optical circuits [21], while the microcavities are filled with silica. We consider compact structures in which all microcavity dimensions are limited to less than 1μm.

We use a two-dimensional finite-difference frequency-domain (FDFD) method [22] to numerically calculate the absorption in the material filling the slit. This method allows us to directly use experimental data for the frequency-dependent dielectric constant of metals such as silver [23], including both the real and imaginary parts, with no approximation. We use perfectly matched layer (PML) absorbing boundary conditions at all boundaries of the simulation domain [24]. We also use the total-field-scattered-field formulation to simulate the response of the structure to a normally incident plane wave input [25].

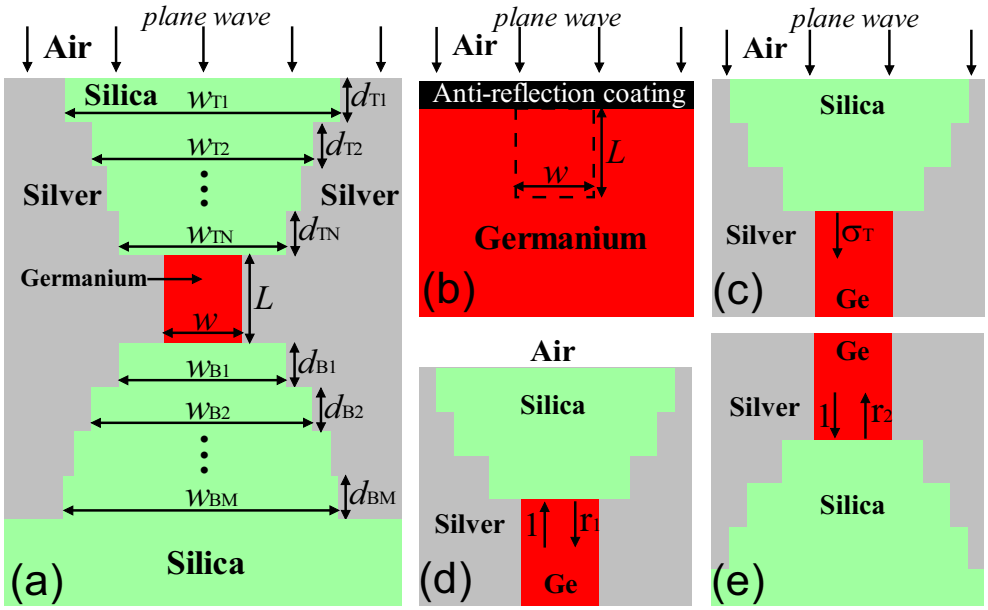

Fig. 1. (a) Schematic of a structure consisting of a slit in a silver film with N microcavities at the entrance side, and M microcavities at the exit side of the slit deposited on a silica substrate. The slit is filled with germanium, while the microcavities are filled with silica. (b) Schematic of a bulk germanium photodetector with an anti-reflection coating. (c) Schematic defining the transmission cross section σ_T of a silver-germanium-silver waveguide through the structure above the entrance side of the slit of Fig. 1(a) for a normally incident plane wave from air. (d) Schematic defining the reflection coefficient r_1 of the fundamental TM mode of a silver-germanium-silver waveguide at the interface of such a waveguide with the structure above the entrance side of the slit of Fig. 1(a). (e) Schematic defining the reflection coefficient r_2 of the fundamental TM mode of a silver-germanium-silver waveguide at the interface of such a waveguide with the structure below the exit side of the slit of Fig. 1(a).

For comparison of different configurations, we define the *absorption cross section* σ_A of the slit as the total light power absorbed by the material (germanium) in the slit, normalized by the incident plane wave power flux [9]. In two dimensions, the cross section is in the unit of length. We also calculate the absorption cross section for the same volume of germanium in a uniform thick slab with an anti-reflection coating, which is a typical configuration for conventional photodetectors [9] (Fig. 1(b)). The ratio between these two absorption cross sections defines the *absorption enhancement factor* η, which is a measure of the enhancement of the light absorption for a unit volume of absorbing material.

#156509 - $15.00 USD Received 13 Oct 2011; revised 8 Dec 2011; accepted 8 Dec 2011; published 15 Dec 2011

We employ single-mode scattering matrix theory to account for the absorption cross section σ_A of the slit in the structure of Fig. 1(a) [26]. We define the transmission cross section σ_T of a silver-germanium-silver metal-dielectric-metal (MDM) waveguide of width w (in the unit of length in two dimensions) as the transmitted power into the waveguide from the structure above the entrance side of the slit of Fig. 1(a), normalized by the incident plane wave power flux (Fig. 1(c)). We also define r_1 (r_2) as the complex magnetic field reflection coefficient for the fundamental propagating TM mode in a silver-germanium-silver MDM waveguide of width w at the interface of such a waveguide with the structure above the entrance side (below the exit side) of the slit of Fig. 1(a) (Figs. 1(d) and 1(e)). We use FDFD to numerically extract σ_T, r_1, and r_2 [26]. The absorption cross section σ_A of the slit can then be calculated using scattering matrix theory as:

$$\sigma_A = \frac{f_{Ge}\sigma_T(1-\left|\exp(-\gamma L)\right|^2)(1+\left|r_2\exp(-\gamma L)\right|^2)}{\left|1-r_1 r_2\exp(-2\gamma L)\right|^2}, \quad (1)$$

where γ is the complex wave vector of the fundamental propagating TM mode in a silver-germanium-silver MDM waveguide of width w, L is the length of the slit, and f_{Ge} is the ratio of the power absorbed in germanium to the total power absorbed in the slit, which also includes the power absorbed in the metal. Based on Eq. (1), we observe that, for fixed slit dimensions, γ, L and f_{Ge} are fixed, so that the absorption cross section σ_A of the slit is solely determined by σ_T, r_1, and r_2. These three parameters in turn can be tuned by adjusting the geometrical dimensions of the microcavities at the entrance and exit sides of the slit.

In addition, the absorption cross section for the same volume of germanium in a conventional bulk photodetector with anti-reflection coating (Fig. 1(b)) is

$$\sigma_{A,bulk} = w(1-\left|\exp(-\gamma_0 L)\right|^2),$$

Where γ_0 is the complex wave vector of a plane wave propagating in germanium. Thus, the absorption enhancement factor for the slit is

$$\eta \equiv \frac{\sigma_A}{\sigma_{A,\text{bulk}}} = \frac{f_{Ge}\sigma_T(1-\left|\exp(-\gamma L)\right|^2)(1+\left|r_2\exp(-\gamma L)\right|^2)}{w(1-\left|\exp(-\gamma_0 L)\right|^2)\left|1-r_1 r_2\exp(-2\gamma L)\right|^2} = \eta_1\eta_2\eta_3, \quad (2)$$

where $\eta_1 \equiv \frac{f_{Ge}(1-\left|\exp(-\gamma L)\right|^2)}{1-\left|\exp(-\gamma_0 L)\right|^2}$, $\eta_2 \equiv \frac{\sigma_T}{w}$, and $\eta_3 \equiv \frac{1+\left|r_2\exp(-\gamma L)\right|^2}{\left|1-r_1 r_2\exp(-2\gamma L)\right|^2}$. We note that η_1 is fixed when the slit dimensions w and L are fixed, and does not depend on the microcavity structures above and below the slit. As an example, for a silver-germanium-silver slit with w = 50 nm, L = 122 nm at λ_0 = 1.55μm we find η_1~1.42. In addition, η_2 is the transmission cross section enhancement factor of the MDM waveguide with respect to its geometrical cross section, associated with the microcavities above the entrance side of the slit. Finally, η_3 is the resonance enhancement factor, associated with the slit resonance. We note that η_3 is a function of the reflection coefficients r_1 and r_2 at both sides of the slit, and therefore depends on both the structure above and the structure below the slit. We also observe that the resonance enhancement factor η_3 is maximized for $|r_1|,|r_2|\to 1$, and when the slit resonance condition $\arg(r_1) + \arg(r_2) - 2\text{Im}(\gamma)L = -2m\pi$ is satisfied, where m is an integer. We note, however, that there is a tradeoff between the resonance enhancement factor η_3, and the transmission cross section enhancement factor η_2. As a result, in the optimized structures we have $|r_1|<1$ in all cases.

#156509 - $15.00 USD Received 13 Oct 2011; revised 8 Dec 2011; accepted 8 Dec 2011; published 15 Dec 2011

3. Results

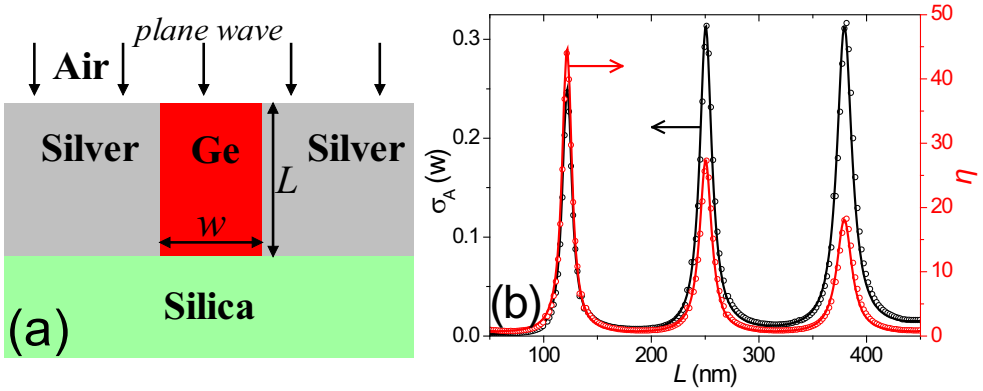

Fig. 2. (a) Schematic of a structure consisting of a single slit in a silver film deposited on a silica substrate. The slit is filled with germanium. (b) Absorption cross section σ_A in units of w (black line and circles), and absorption enhancement factor η (red line and circles) for the structure of Fig. 2(a) as a function of slit length L calculated using FDFD (circles) and scattering matrix theory (solid line). Results are shown for w = 50nm and λ_0 = 1.55μm.

Table 1. Absorption enhancement factor η, transmission cross section enhancement factor η_2, resonance enhancement factor η_3, and reflection coefficients r_1, r_2. Also shown is the absorption cross section σ_A in units of w, calculated using scattering matrix theory and FDFD. Results are shown for the optimized structures of Fig. 1(a) with (N, M) = (0, 0), (1, 0), (1, 1), and (2, 2).

(n, M)	(0, 0)	(1, 0)	(1, 1)	(2, 2)
η	43.9	75.7	133.6	410.6
H_2	0.96	2.98	1.87	2.96
H_3	32.3	17.9	50.4	97.9
R_1	0.940exp(i*3.02)	0.819exp(i*3.04)	0.887exp(i*3.14)	0.924exp(i*3.10)
R_2	0.889exp(i*2.91)	0.889exp(i*2.91)	0.972exp(i*2.86)	0.998exp(i*2.91)
σ_A (w) S-Matrix	0.250	0.416	0.744	2.299
σ_A (w) FDFD	0.246	0.423	0.747	2.295

We first consider our reference structure consisting of a single subwavelength slit in a metal film deposited on a substrate (Fig. 2(a)). In Fig. 2(b), we show the absorption cross section σ_A, and the absorption enhancement factor η for the structure of Fig. 2(a) as a function of the slit length L calculated using FDFD. We observe that, as the slit length L increases, both the absorption cross section and the absorption enhancement factor exhibit peaks, corresponding to the Fabry-Pérot resonances in the slit. In Fig. 2(b) we also show σ_A and η calculated using scattering matrix theory (Eqs. (1), (2)). We observe that there is excellent agreement between the scattering matrix theory results and the exact results obtained using FDFD. Similarly, excellent agreement between the results of these two methods is observed for all the structures considered in this paper (Table 1). The maximum absorption enhancement factor η of ~43.9 with respect to a conventional photodetector is obtained at the first peak (L = 122nm), due to the strong electromagnetic field enhancement associated with the Fabry-Pérot resonance in the slit [10]. For such a structure, the transmission cross section enhancement factor is η_2~0.96 (Table 1). In other words, the transmission cross section of a silver-germanium-silver MDM waveguide with w = 50 nm at λ_0 = 1.55μm is approximately equal to its geometrical cross section. In addition, the resonance enhancement factor is η_3~32.3 (Table 1). Such large resonance enhancement is due to the strong reflectivities r_1, r_2 at both sides of the slit (Table 1), associated with the strong impedance mismatch between the

#156509 - $15.00 USD Received 13 Oct 2011; revised 8 Dec 2011; accepted 8 Dec 2011; published 15 Dec 2011

fundamental MDM mode in the slit and propagating plane waves in air and in the silica substrate [9].

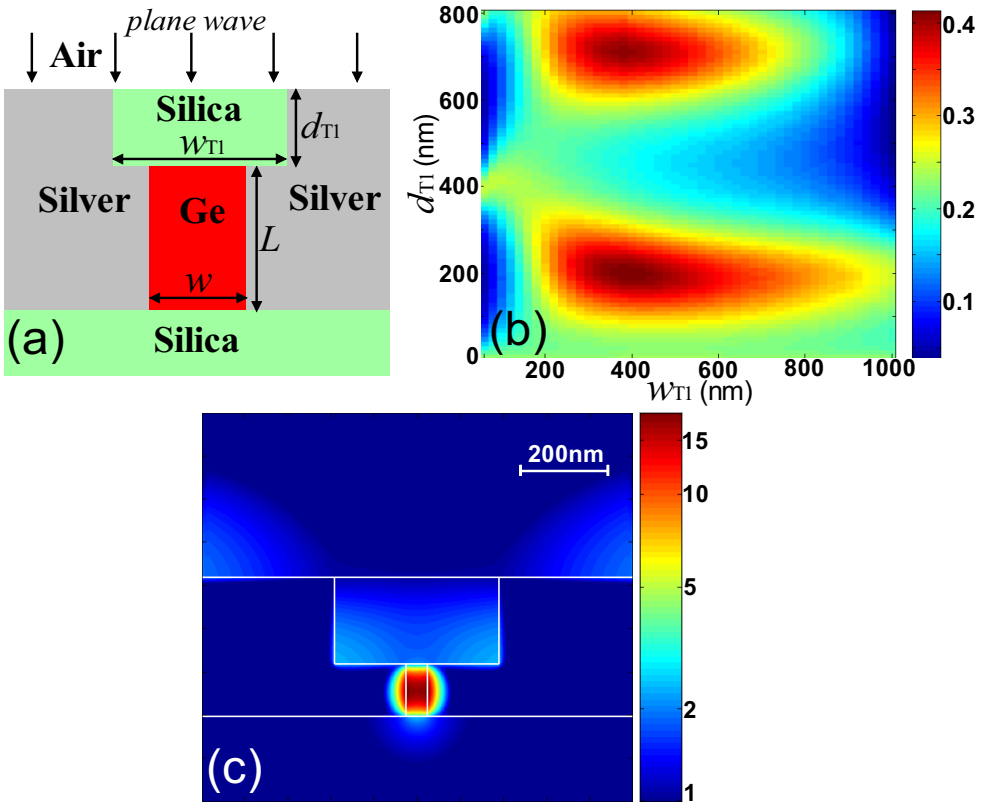

Fig. 3. (a) Schematic of a structure consisting of a slit in a silver film deposited on a silica substrate with a single microcavity at the entrance side of the slit. The slit is filled with germanium, while the microcavity is filled with silica. (b) Absorption cross section σ_A in units of w for the structure of Fig. 3(a) as a function of width w_{T1} and length d_{T1} of the microcavity calculated using FDFD. Results are shown for w = 50nm, L = 122nm, and λ_0 = 1.55μm. (c) Profile of the magnetic field amplitude enhancement with respect to the field amplitude of the incident plane wave for the structure of Fig. 3(a) for w_{T1} = 380nm and d_{T1} = 200nm. All other parameters are as in Fig. 3(b).

We next consider a structure consisting of a slit in a metal film with a single microcavity at the entrance side of the slit (Fig. 3(a)). In Fig. 3(b), we show the absorption cross section σ_A for the structure of Fig. 3(a) as a function of the width w_{T1} and length d_{T1} of the microcavity. For the range of parameters shown, we observe two absorption peaks associated with different resonant modes of the microcavity. When the microcavity dimensions approach a resonance, the light power collected by the microcavity increases, and the coupling to the slit is enhanced. However, we found that the maximum absorption cross section in the slit is not obtained when the microcavity is on resonance. This is due to the fact that the on resonance field pattern in the microcavity is a standing wave, which does not correspond to optimum coupling to the slit [20]. The maximum absorption cross section of σ_A~0.423w is obtained for such a structure at w_{T1} = 380nm and d_{T1} = 200nm, and the corresponding absorption enhancement factor is η~75.7 (Table 1). We observe that for such a structure the transmission cross section enhancement factor is η_2~2.98 (Table 1), which is ~3.1 times larger compared to a slit without the microcavity. In other words, the microcavity can greatly enhance the coupling of the incident light into the slit mode, by improving the impedance matching between the incident plane wave and the slit mode. On the other hand, the resonance enhancement factor for the optimized structure of Fig. 3(a) is η_3~17.9 (Table 1), which is ~1.8

#156509 - $15.00 USD Received 13 Oct 2011; revised 8 Dec 2011; accepted 8 Dec 2011; published 15 Dec 2011

times smaller than the one of a slit without a microcavity. This is due to the fact that the reflectivity $|r_1|^2$ at the interface between the silver-germanium-silver slit and the silver-silica-silver microcavity is smaller than the one at the interface between the silver-germanium-silver slit and air (Table 1). Thus, overall the use of an optimized single microcavity at the entrance side of the slit (Fig. 3(a)) results in $3.1/1.8 \simeq 1.7$ times larger absorption cross section compared to the optimized reference slit without a microcavity (Fig. 2(a)). In Fig. 3(c), we show the magnetic field profile for the structure of Fig. 3(a) with dimensions optimized for maximum absorption cross section σ_A. We observe that the field in the microcavity is weaker than the field in the slit. The maximum magnetic field amplitude enhancement in the slit with respect to the incident plane wave is ~18 (Fig. 3(c)).

We next consider a structure with a single microcavity at each of the entrance and exit sides of the slit (Fig. 1(a) with $N = M = 1$). We use a genetic global optimization algorithm in combination with FDFD [27,28] to optimize the width and length of both microcavities in the structure for maximum absorption cross section σ_A. All microcavity dimensions are limited to less than 1μm. The maximum absorption cross section for such a structure is found to be $\sigma_A \sim 0.747w$, and the corresponding absorption enhancement factor is $\eta \sim 133.6$ (Table 1). Similar to the optimized ($N = 1$, $M = 0$) structure (Fig. 3(a)), the microcavity at the entrance side of the slit results in larger (by a factor of ~1.95) transmission cross section enhancement factor η_2, and smaller reflectivity $|r_1|^2$ compared to a slit without microcavities (Table 1). However, the presence of a microcavity at the exit side of the slit for the ($N = 1$, $M = 1$) structure results in larger reflectivity $|r_2|^2$ compared to a slit without a microcavity (Table 1). This is due to the fact that such a cavity can be tuned to either resonantly enhance or resonantly suppress the reflectivity. In the optimized ($N = 1$, $M = 1$) structure, resonant enhancement of the reflectivity $|r_2|^2$ is achieved by proper choice of the microcavity length d_{B1}. The increase of the reflectivity $|r_2|^2$ at the exit side of the slit for the optimized ($N = 1$, $M = 1$) structure overcompensates the decrease of the reflectivity $|r_1|^2$ at the entrance side, so that its resonance enhancement factor $\eta_3 \sim 50.4$ (Table 1) is ~1.5 times larger than the one of a slit without a microcavity. Thus, the use of a single microcavity at both the entrance and exit sides of the slit enables increasing both the transmission cross section enhancement factor η_2, and the resonance enhancement factor η_3. Overall, such a structure, when optimized, results in $1.95 \times 1.5 \simeq 3$ times larger absorption cross section compared to the optimized reference slit without microcavities (Fig. 2(a)).

To further enhance the absorption cross section of the slit, we consider structures with multiple microcavities at both the entrance and exit sides of the slit (Fig. 1(a)). More specifically, we use the genetic optimization algorithm to optimize the widths and lengths of all microcavities in a ($N = 2$, $M = 2$) structure. As before, the dimensions of the structures at both the entrance and the exit sides of the slit are limited to less than 1μm. The maximum absorption cross section for such a structure is found to be $\sigma_A \sim 2.295w$, and the corresponding absorption enhancement factor is $\eta \sim 410.6$ (Table 1). We observe that the use of multiple microcavities at the entrance side of the slit ($N = 2$, $M = 2$) increases the transmission cross section enhancement factor η_2 compared to the single microcavity ($N = 1$, $M = 1$) structure (Table 1). This is due to the fact that multiple-section structures can improve the impedance matching and therefore the coupling between optical modes [28]. In addition, the use of multiple microcavities at the entrance and exit sides of the slit ($N = 2$, $M = 2$) also increases the corresponding reflectivities $|r_1|^2$ and $|r_2|^2$ compared to the single microcavity ($N = 1$, $M = 1$) structure (Table 1). Thus, a large resonance enhancement factor $\eta_3 \sim 97.9$ is obtained (Table 1). This is due to the fact that multiple-section structures can be more finely tuned than single-section structures, and can therefore provide larger resonantly enhanced reflectivity. This is analogous to the multilayer Bragg reflectors which can provide larger reflectivity compared to single layer structures. Overall, the optimized ($N = 2$, $M = 2$) structure results in ~3.1 times larger transmission cross section enhancement factor η_2, ~3 times larger resonance enhancement factor η_3, and therefore ~9.3 times larger absorption cross section compared to the optimized reference slit without microcavities (Fig. 2(a)).

#156509 - $15.00 USD Received 13 Oct 2011; revised 8 Dec 2011; accepted 8 Dec 2011; published 15 Dec 2011

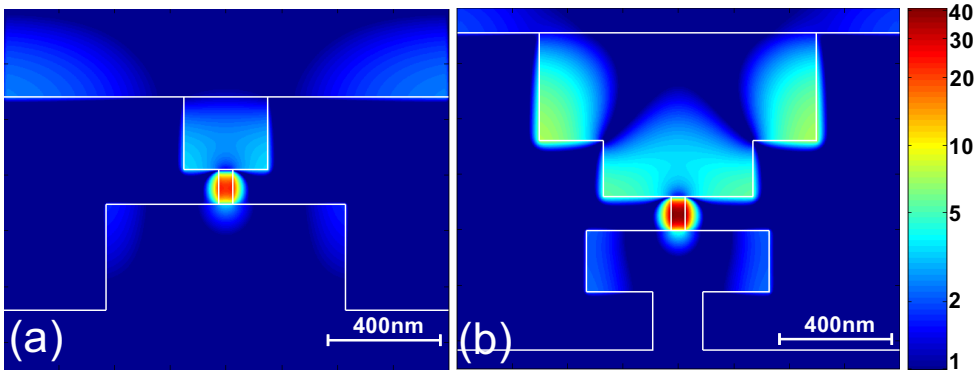

Fig. 4. (a) Profile of the magnetic field amplitude enhancement with respect to the field amplitude of the incident plane wave for the optimized structure of Fig. 1(a) with $N = M = 1$. Results are shown for (w_{T1}, d_{T1}, w_{B1}, d_{B1}) = (300, 260, 860, 380) nm. All other parameters are as in Fig. 3(b). (b) Profile of the magnetic field amplitude enhancement with respect to the field amplitude of the incident plane wave for the optimized structure of Fig. 1(a) with $N = M = 2$. Results are shown for (w_{T1}, d_{T1}, w_{T2}, d_{T2}, w_{B1}, d_{B1}, w_{B2}, d_{B2}) = (1000, 390, 540, 200, 660, 220, 180, 210) nm. All other parameters are as in Fig. 3(b).

In Figs. 4(a) and 4(b), we show the magnetic field profile for the ($N = 1$, $M = 1$) and ($N = 2$, $M = 2$) cases, respectively, with dimensions optimized for maximum absorption cross section σ_A. We find that, as the number of microcavities increases, the field in the microcavities at the entrance side is stronger, due to the fact that more incident light is collected in the microcavities. The maximum magnetic field amplitude enhancement in the slit with respect to the incident plane wave is ~23 and ~40 for the ($N = 1$, $M = 1$) and ($N = 2$, $M = 2$) cases, respectively.

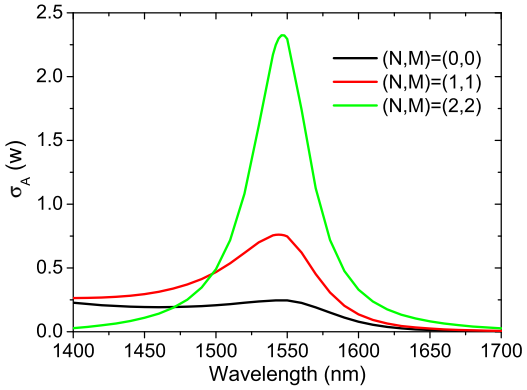

Fig. 5. Absorption cross section σ_A in units of w as a function of wavelength for the optimized structures of Fig. 1(a) with $N = M = 0$ (black line), $N = M = 1$ (red line), and $N = M = 2$ (green line). All other parameters for the $N = M = 0$, $N = M = 1$, and $N = M = 2$ cases are as in Figs. 3(b), 4(a), and 4(b), respectively.

The microcavity-enhanced structures were optimized at a single wavelength of λ_0 = 1.55μm. In Fig. 5, we show the absorption cross section σ_A as a function of incident wavelength for the optimized structures of Fig. 2(a) ($N = M = 0$), Fig. 4(a) ($N = M = 1$), and Fig. 4(b) ($N = M = 2$). We observe that the operation wavelength range for high absorption is broad. For example, the full width at half maximum (FWHM) of the absorption peak in the ($N = M = 2$) case is ~50nm. This is due to the fact that in all cases the enhanced absorption is not associated with any strong resonances. In other words, the quality factors Q of the microcavities are low.

#156509 - $15.00 USD Received 13 Oct 2011; revised 8 Dec 2011; accepted 8 Dec 2011; published 15 Dec 2011

4. Conclusions

In this paper, we investigated compact submicron structures consisting of multiple optical microcavities at both the entrance and exit sides of a subwavelength plasmonic slit filled with an absorbing material, with the goal to increase the absorption in the slit. Our reference structure consisted of a single subwavelength slit in a metal film deposited on a substrate. For such a structure, the maximum absorption enhancement factor with respect to a conventional photodetector is η~43.9, and the absorption enhancement is due to the large resonant field enhancement in the slit, associated with the strong reflectivities at both sides of the slit.

To further enhance the absorption in the slit, we first considered a structure with a single microcavity at the entrance side of the slit. We found that the microcavity greatly enhances the coupling of the incident light into the slit, by improving the impedance matching between the incident plane wave and the slit mode. On the other hand, the microcavity reduces the reflectivity at the entrance side of the slit, and therefore the resonance enhancement factor. Overall, the use of an optimized single microcavity at the entrance side of the slit resulted in an absorption enhancement factor of η~75.7, which is ~1.7 times larger compared to the slit without a microcavity. We then considered a structure with a single microcavity at each of the entrance and exit sides of the slit. We found that the microcavity at the exit side of the slit results in larger reflectivity, and therefore larger resonant field enhancement. Overall, the use of an optimized single microcavity at both the entrance and exit sides of the slit resulted in an absorption enhancement factor of η~133.6 which is ~3 times larger compared to the slit without a microcavity.

We finally considered structures with multiple microcavities at both the entrance and exit sides of the slit. We found that the use of multiple microcavities at the entrance side of the slit further enhances the coupling of the incident light into the slit through improved impedance matching. In addition, the use of multiple microcavities at the entrance and exit sides of the slit also increases the reflectivities at both sides of the slit, and therefore the resonant field enhancement. Overall, the use of two optimized microcavities at both the entrance and exit sides of the slit resulted in an absorption enhancement factor of η~410.6 which is ~9.3 times larger compared to the slit without a microcavity. We also found that, while the microcavity-enhanced structures were optimized at a single wavelength, the operation wavelength range for high absorption is broad.

As final remarks, we note that for the fabrication of each microcavity of the structure, one can make first a silica ridge using lithography and etching processes. This step can then be followed by metal deposition and lift-off processes to form the metal parts of the microcavity [9].

Acknowledgments

This research was supported by the Louisiana Board of Regents (contracts LEQSF(2009-12)-RD-A-08 and NSF(2010)-PFUND-187), and the National Science Foundation (Award No. 1102301).

#156509 - $15.00 USD Received 13 Oct 2011; revised 8 Dec 2011; accepted 8 Dec 2011; published 15 Dec 2011